Check for
updates

Progress Toward Fast Decay Energy Spectroscopy for Actinide Analysis

Nathan Hines[1] · S. T. P. Boyd[2] · Geon-Bo Kim[1]

Abstract

Decay energy spectroscopy (DES) is an increasingly popular technique for measuring isotopic composition of actinide samples for nuclear safeguards applications. Current approaches for actinide DES utilize milligram-scale external gold absorbers (> 0.1 nJ/K) that are integrated with actinide samples through mechanical kneading and are thermally connected to microcalorimeters using indium or gold wire bonds. This leads to relatively slow sensor rise time and, consequently, limits counting speed to a few counts per second. We are developing faster metallic magnetic calorimeter-based DES by integrating actinide samples with magnetic sensor materials. This reduces signal rise time and enables high counting speed while maintaining the ability to knead the radioactive source with the absorber. We have measured signal rise time of 0.7 μs with a 1.5 mg external gold absorber using this approach. We also demonstrated online DES operation using an Ortec DSPEC 50, a commercially available data acquisition system developed for semiconductor detectors.

1 Introduction

Accurate analysis of nuclear material composition is critical for nuclear safeguards. The current state-of-the-art method for analyzing nuclear samples is a combination of thermal-ionization mass spectrometry (TIMS) and alpha spectroscopy [1]. While this technique is precise, development of an independent analysis method is highly desired to improve reliability of nuclear material accountancy [2]. Decay energy spectroscopy (DES) is a promising, complementary technique

---

✉ Geon-Bo Kim
   kim90@llnl.gov

1   Lawrence Livermore National Laboratory, Livermore, CA 94550, USA

2   University of New Mexico, Albuquerque, NM 87131, USA

for measuring nuclear material composition that identifies and quantifies radioactive nuclides by measuring temperature increase resulting from radioactive decay [3]. Nuclear samples are encapsulated by a gold foil (referred to as the absorber), mechanically kneaded with the absorber, then thermally connected to a microcalorimeter sensor, such as a metallic magnetic calorimeter (MMC) or transition-edge sensor (TES) [4, 5].

Actinide DES for nuclear safeguards applications has several important considerations. First, a relatively large mass of radioactive material needs to be analyzed due to their long half-lives. For example, U-238 has a half-life and specific activity of 4.5 billion years and 12,400 decays per second per gram, respectively. Hence, isotopic analysis of a typical uranium nuclear safeguards sample requires 100 s of micrograms to be analyzed if a result is desired within the several hours available in a single magnetization cycle of an adiabatic demagnetization refrigerator. Consequently, large absorbers must be used to encapsulate the sample. Second, the absorbers are typically mounted separate from and externally coupled to the microcalorimeter. This allows samples to be routinely replaced by technicians while the microcalorimeter remains in the experimental setup. Various ways of sample attachment have been developed that provide both high-energy resolution and simple, repeatable sample attachment [6–8]. Third, actinides should be completely encapsulated by and mechanically kneaded into absorber foils to improve energy resolution [7]. Figure 1 shows our standard MMC-based DES implementation in which gold wire bonds are used to attach the absorber to the MMC. 10 to 90% signal rise time was limited to order 100 μs at 20 mK, which is consistent with previous reports [6]. While this rise time is sufficient for low-activity samples, both nuclear safeguards and forensics applications can greatly benefit from the ability to process higher count-rate samples. Examples include quicker isotopic ratio determination, reduction of uncertainties due to counting statistics, and the ability to process samples containing high-activity nuclear fission products.

We are developing new approaches for routine actinide DES that significantly improve counting speed over current implementations. Absorbers are integrated with paramagnetic sensors to improve thermal coupling. We present two techniques for improving MMC speed and compare them to our standard approach.
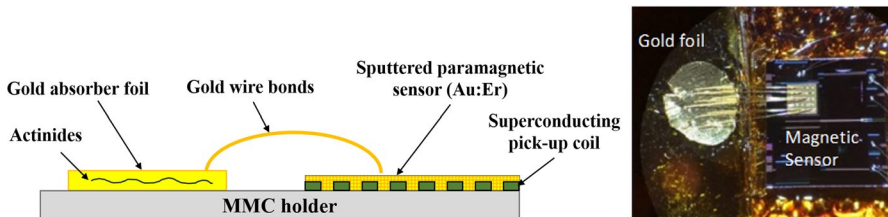

Fig. 1 *Left:* Schematic drawing of a conventional DES method. The absorber foil is connected to the MMC sputtered paramagnetic sensor via several gold wire bonds. *Right:* A photograph of a DES setup. Signal rise time in this configuration is limited by the time required for heat to flow between the sample and paramagnet
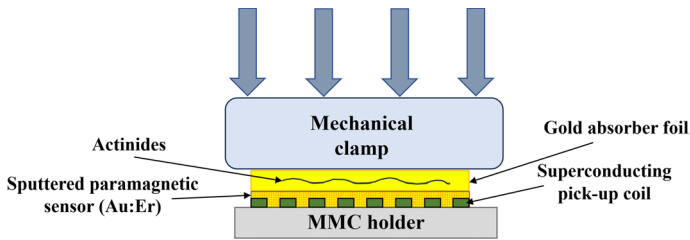
Fig. 2 Method 1 places the absorber onto the MMC's sputtered paramagnet. No wire bond or indium thermal connections are needed in this configuration as the clamp thermally couples the sample to the MMC
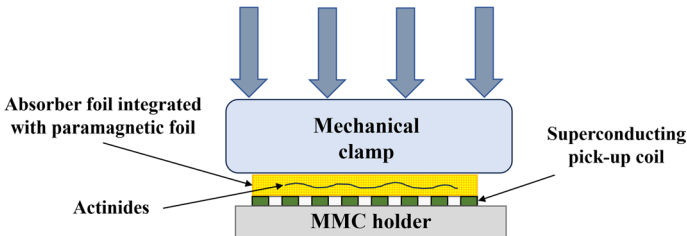

Fig. 3 Method 2 integrates the absorber with a paramagnetic foil, then places it onto an MMC bare pickup coil. Note that the MMC does not have a sputtered paramagnet in this configuration

2 MMC-based DES Configurations

2.1 Method 1

This configuration mechanically presses the gold absorber against the Au:Er or Ag:Er sputtered paramagnetic sensor. This pressure contact thermally connects the absorber to the MMC via conduction electrons by Wiedemann–Franz law [9]; thus, boundary thermal resistance can be minimal and fast signal readout can be achieved. A clamp provides the force needed for the pressure contact, as shown in Fig. 2. Challenges include unknown thermal conductance of the mechanical contact at low temperatures and risk of cross contaminating the MMC surface by improperly encapsulated actinide samples.

2.2 Method 2

This technique laminates the absorber with a paramagnetic foil using a roll mill. Next, the laminated package is placed directly onto an MMC superconducting pickup coil that has no sputtered paramagnet layer, as shown in Fig. 3. This provides better integration of the absorber to the paramagnetic sensor and fast sensor response time [10]. Challenges to this method include synthesizing magnetic foils
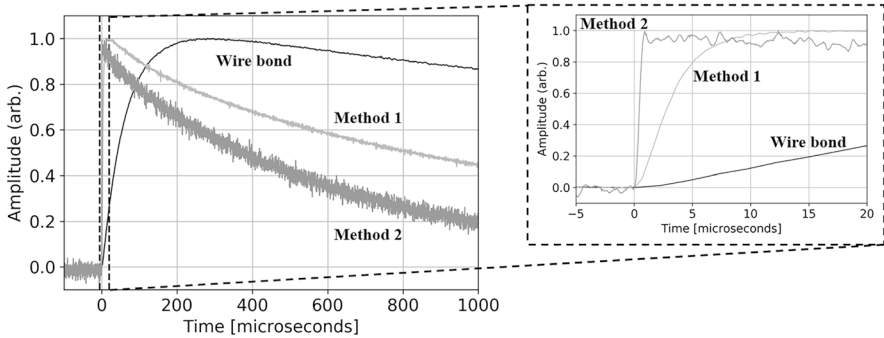
Fig. 4 Raw pulses from three MMC-based DES implementations. Rise times associated with Method 1 and 2 resulted in ~20× and ~170× shorter rise times, respectively, when compared with our standard DES implementation. Visual noise difference is primarily due to different sampling rates

Table 1 Measured rise times and associated experimental conditions

Method	Rise time	Temp	Absorber mass	Heat capacity
Wire bond	120 μs	20 mK	2 mg	0.13 nJ/K
1	6 μs	20 mK	3 mg	0.20 nJ/K
2	0.7 μs	20 mK	1.5 mg	0.10 nJ/K

free of magnetic contamination and inconsistent paramagnet-pickup coil coupling due to non-negligible gaps between the sensor and pickup coil.

3 Results

Figure 4 shows a comparison of signals measured from three DES configurations: wire bond, Method 1, and Method 2. As shown in Table 1, Method 1 resulted in greater than an order of magnitude reduction in signal rise time when compared to our wire-bond technique. This result was reproducible in multiple experiments. Rise time associated with Method 2 was nearly an order of magnitude shorter than that of Method 1. To first order, signal decay time is a function of thermal conductance between the absorber and thermal bath, which differed for each pulse shown in Fig. 4. Future studies will work to decrease decay time and make heat sinking more consistent.

The Method 2 configuration results in sub-microsecond signal rise time, which is similar to that of large-volume high-purity germanium (HPGe) semiconductor gamma-ray detectors. This enables use of commercial-off-the-shelf (COTS) data acquisition systems for pulse processing with trapezoidal filtering [11]. Trapezoidal filtering is preferred for fast counting experiments due to its short signal integration time, fewer pileup events, and consequently, less detector dead time when compared to Weiner optimal filtering [12]. A preliminary implementation of the Method 2 MMC configuration exposed an external Gd-148 alpha-emitting source
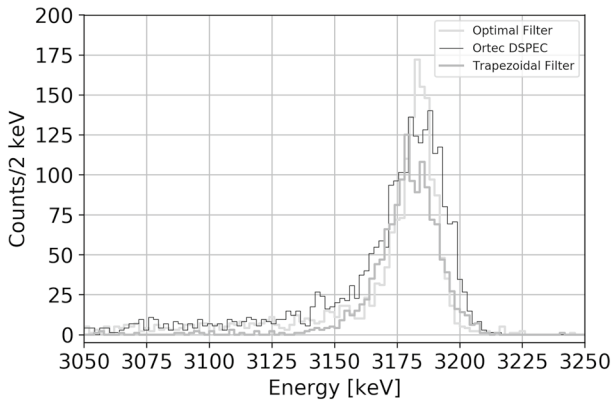
Fig. 5 Three pulse-processing techniques were used to analyze Gd-148 alpha-decay measurements that utilized a Method 2 configuration. Trapezoidal (*dark gray*) and optimal (*light gray*) filters were used for offline data analysis, while an Ortec DSPEC 50 (*black*) was used for online spectroscopy

to a paramagnetic foil mounted upon a bare MMC pickup coil [10]. Data from this experiment were filtered using three methods to the produce pulse-height spectra shown in Fig. 5. Histograms shown in light gray and dark gray were generated by offline processing of raw, triggered pulses, and utilized Weiner optimal and trapezoidal filtering techniques, respectively. Offline trapezoidal shaping rise and flat-top times were 20 and 1 microseconds, respectively. Data shown in black correspond to online pulse processing using a DSPEC 50 HPGe digital signal processing unit. Rise and flat-top times for online analysis were 14 and 1 microsecond, respectively. Weiner optimal filtering resulted in a full width at half-maximum (FWHM) energy resolution of 16.4 keV. Offline trapezoidal filtering and DSPEC 50 energy resolution were 24.1 and 26.6 keV, respectively. As expected, DSPEC 50 and offline trapezoidal filtering resulted in similar energy resolution.

4 Conclusion and Discussion

We have demonstrated two methods for decreasing signal rise time in DES MMCs. Direct clamping of the actinide absorber to the MMC sputtered paramagnet produced a signal rise time of ~ 6 microseconds, while integrating the actinide absorber directly with a paramagnetic foil resulted in a 0.7-microsecond rise time. Signal throughput is fundamentally limited by rise time because decay time can be adjusted, though it cannot be faster than the rise time. Hence the techniques presented in this work indicate that signal throughput can be increased by over an order of magnitude when compared to our current MMC-based DES implementation. The result is directly applicable and beneficial to both nuclear safeguards and forensics. Additionally, faster MMC response time benefits pulse-shape discrimination efforts associated with the MAGNETO-DM dark matter experiment

and can mitigate pulse-pileup effects that distort the high-statistics beta-decay spectrum measured in the MAGNETO-υ sterile neutrino experiment [13, 14].

Future work will include shortening signal decay time, as this parameter must also be decreased to enable analysis of high-activity samples. Temperature stability and energy resolution will be improved to enable plutonium isotopic analysis. Lastly, use of COTS digital acquisition systems will continue to be explored, as this capability makes MMC-based DES more user-friendly.

Author contributions N. H. wrote the main manuscript, conducted the experiments discussed in the text, and performed data analysis shown in Fig. 4.G. K. is the principal investigator for this project. He guided experimental efforts, performed data analysis for Fig. 5, and provided background and context for the manuscript.S. B. performed proof-of-concept calculations and simulations for this work and provided guidance for experiments. He also assisted in interpretating data measured in this work. All authors reviewed the manuscript.

Declarations

Conflict of interests The authors declare no competing interests.

References

1. K. Zhao et al., IAEA Department of Safeguards, IAEA-STR-368 (2010)
2. G. Kim et al., Symposium on International Safeguards: Reflecting on the Past and Anticipating the Future (2022)
3. K. Koehler, Appl. Sci. **11**(9), 4044 (2021). https://doi.org/10.3390/app11094044
4. A. Fleischmann, C. Enss, G.M. Seidel, *Cryogenic Particle Detection* (Springer, Heidelberg, 2005), pp.151–216. https://doi.org/10.1007/10933596_4
5. K.D. Irwin, G.C. Hilton, *Cryogenic Particle Detection* (Springer, Berlin, 2005), pp.63–150. https://doi.org/10.1007/10933596_3
6. W. Yoon et al., J. Low Temp. Phys. **167**, 280–285 (2012). https://doi.org/10.1007/s10909-012-0539-1
7. A. Hoover et al., Anal. Chem. **87**(7), 396–400 (2015). https://doi.org/10.1021/acs.analchem.5b00195
8. Y. Jang et al., Appl. Radiation Isot. **70**(9), 2255–2259 (2012). https://doi.org/10.1016/j.apradiso.2012.02.109
9. R. Franz, G. Wiedemann, Ueber die wärme-leitungsfähigkeit der metalle. Ann. Phys. **165**(8), 497–531 (1853)
10. S. Boyd et al., IEEE Trans. Appl. Supercond. **33**, 5 (2023). https://doi.org/10.1109/TASC.2023.3259334
11. V. Jordanov et al., NIM A **353**, 261–264 (1994). https://doi.org/10.1016/0168-9002(94)91652-7
12. A. Szymkowiak et al., J. Low Temp. Phys. **93**, 281–285 (1993). https://doi.org/10.1007/BF00693433
13. G. Kim, 18th International Conference on Topics in Astroparticle and Underground Physics (2023)

14.   G. Kim, The 14th UCLA Symposium on Dark Matter (2023)